

**UNIVERSITY OF BUCHAREST**

**Semiclassical and Boson  
Descriptions of the Wobbling  
Motion in Odd-A Nuclei**

Robert Poenaru

Faculty of Physics

March 2022

## *Abstract*

Nova.

**Keywords:** *nuclear shape, nuclear deformation, collective parameters, triaxiality, wobbling.*

## *Acknowledgements*

Nova.

**Keywords:** Thank you!

# Contents

<b>Abstract</b>	<b>i</b>
<b>Acknowledgements</b>	<b>ii</b>
<b>1 Introduction</b>	<b>1</b>
<b>2 Deformed Nuclei</b>	<b>3</b>
2.1 Nuclear deformation . . . . .	3
2.1.1 Collective coordinates . . . . .	3
2.1.2 Nuclear radius under rotation . . . . .	4
2.1.3 Multipole deformations . . . . .	5
2.1.4 Quadrupole Deformation . . . . .	6
2.1.4.1 Axial quadrupole deformations . . . . .	9
2.1.4.2 Non-Axial quadrupole deformations . . . . .	11
2.1.4.3 Lund Convention . . . . .	13
2.1.4.4 Alternative description of the quadrupole deformation . . . . .	13
2.1.5 Nuclear Shapes and Softness . . . . .	15
<b>3 Nuclear Models</b>	<b>18</b>
3.1 Introduction . . . . .	18
3.1.1 Shell model . . . . .	18

# Chapter 1

## Introduction

Ground-state nuclear shapes with spherical symmetry or axial symmetry are predominant across the chart of nuclides. Near closed shells, the deformation is indeed sufficient that models based on spherical symmetries can be used to describe nuclear properties (e.g., energies, quadrupole moments, and so on). Besides the spherical and axially-symmetric shapes, the existence of triaxial nuclear deformation was theoretically predicted a long time ago [1]. The rigid triaxiality of nuclei is defined by the asymmetry parameter  $\gamma$ , giving rise to unique quantum phenomena (this parameter will be characterized later on). The quantum mechanical properties of the rigid triaxial shapes drew a lot of attention within the nuclear physics community lately, since the description of nuclear properties for the deformed nuclei represents a great challenge from both an experimental and a theoretical standpoint (e.g., great progress for the experimental evidence of strong nuclear deformation has only been possible after the 2000s). It is worth mentioning that some experiments concerning alpha-alpha particle reactions induced in heavy nuclei in the early 1960s (e.g., [2]) helped to produce decent amount of data related to the rotational in the high-spin region ( $\geq 20\hbar$ ). Within the experimental studies made by Morinaga et al., the alpha reactions which were induced in the nuclei were generated by the formation of a so-called *compound nucleus*. This system may exist at a large spin value due to the absorption of the angular momentum from the incident particle (i.e., spin values up to  $\approx 25 \hbar$  can be obtained from a 50 MeV alpha particle energy - relative to the target nucleus [2]).

The physics of *high-spin* states have been studied from the early 1950s, with the major breakthrough on the theoretical side made by Bohr and Mottelson [1].

The elusive properties of nuclear rotation were described in terms of the rotational degrees of freedom associated with other nuclear degrees of freedom (e.g., particle-vibration, quadrupole-quadrupole, parity, and so on).

# Chapter 2

## Deformed Nuclei

### 2.1 Nuclear deformation

Most of the nuclei across the nuclide chart are spherical or symmetric in their ground state. Moreover, for the axially symmetric nuclei (i.e, either *oblate* or *prolate*), there is a prolate over oblate dominance.

The spherical shell model only describes nuclei near the closed shells. On the other side, for the nuclei that lie far from closed shells, a deformed potential must be employed.

In the case of even-even nuclei, unique band structures resulting from the vibrations and rotations of the nuclear surface (as proposed by Bohr and Mottelson [1] in the *Geometric Collective Model - GCM*) appear in the energy range 0-2 MeV.

Within the GCM, the nucleus is described as a classical charged liquid drop. For the low-lying energy spectrum, usually, the compression of nuclear matter and the nuclear skin thickness are neglected. This results in the final picture of a liquid drop with a constant nuclear density and a sharp surface [3].

#### 2.1.1 Collective coordinates

The nuclear surface can be described via an expansion of the spherical harmonic functions, with some time-dependent parameters as *expansion coefficients*. The

expression of the nuclear shape is shown below [3]:

$$R(\theta, \varphi, t) = R_0 \left( 1 + \sum_{\lambda=0}^{\infty} \sum_{-\lambda}^{\lambda} \alpha_{\lambda\mu}(t) Y_{\lambda}^{\mu}(\theta, \varphi) \right) . \quad (2.1)$$

In 2.1,  $R$  denotes the nuclear radius as a function of the spherical coordinates  $\theta, \varphi$  expressing the direction, and the time  $t$ , while  $R_0$  is the radius of the spherical nucleus when all the expansion coefficients vanish. It is worth mentioning that the expansion coefficients  $\alpha_{\lambda\mu}$  act as *collective coordinates*, since the time-dependent amplitudes describe the vibrations of the nuclear surface.

### 2.1.2 Nuclear radius under rotation

To get a grasp at the physical meaning behind the deformation parameters that are used to describe the nuclear surface, it is instructive to see what happens when the system undergoes a rotation transformation.

The function  $R(\theta, \varphi)$  describes the original (non-rotated) nuclear shape. Rotating the system will result in the change of the angular coordinates  $(\theta, \varphi)$  to  $(\theta', \varphi')$ , which will correspond to a new function  $R'(\theta', \varphi')$ . Moreover, both nuclear surfaces (i.e., the non-rotated and the rotated one) must hold the equality:

$$R'(\theta', \varphi') = R(\theta, \varphi) \quad (2.2)$$

The rotational invariance of  $R$  employs that  $R'(\theta, \varphi)$  must have the same functional form, but the expansion coefficients  $\alpha_{\lambda\mu}$  must be rotated, meaning:

$$\sum_{\lambda\mu} \alpha'_{\lambda\mu} Y'_{\lambda\mu}(\theta, \varphi) = \sum_{\lambda\mu} \alpha_{\lambda\mu} Y_{\lambda\mu}(\theta, \varphi) . \quad (2.3)$$

Note that in Eq. 2.3, the spherical harmonics  $Y'_{\lambda\mu}$  are obtained via the usual rotation matrices. Finally, the invariance of Eq. 2.1 is achieved if the set of parameters  $\alpha_{\lambda\mu}$  transform similarly to a *spherical tensor with angular momentum*  $\lambda$  [4], that is:

$$\alpha'_{\lambda\mu} = \sum_{\mu'} \mathcal{D}_{\mu\mu'}^{(\lambda)} \alpha_{\lambda\mu'} . \quad (2.4)$$

Besides the spherical tensor character, the collective coordinates also have the following properties (emerging from Eq. 2.1):

- Complex Conjugation.

$$Y_{\lambda\mu}^*(\theta, \varphi) = (-1)^\mu Y_{\lambda-\mu}(\theta, \varphi), \quad (2.5)$$

$$\alpha_{\lambda\mu}^* = (-1)^\mu \alpha_{\lambda-\mu}. \quad (2.6)$$

- Parity - the coordinates  $\alpha_{\lambda\mu}$  must undergo the same change of sign under a parity transformation as the spherical harmonics, in order to keep the invariance of the nuclear surface.

$$(r, \theta, \varphi) \xrightarrow{P} (r, \pi - \theta, \pi + \varphi), \\ Y_{\lambda\mu}(\theta, \varphi) \xrightarrow{P} Y_{\lambda\mu}(\pi - \theta, \pi + \varphi) = (-1)^\lambda Y_{\lambda\mu}(\theta, \varphi).$$

Therefore, the parity of the expansion coefficients are:

$$\pi(\alpha_{\lambda\mu}) = (-1)^\lambda. \quad (2.7)$$

### 2.1.3 Multipole deformations

In the expansion of the nuclear surface defined by Eq. 2.1, the different values for  $\lambda$  will determine different effects regarding the physical aspects of the nucleus. As such, the first values of  $\lambda$  will be examined in terms of the physical meaning.

**Monopole mode** This corresponds to the first value of  $\lambda = 0$ . This is the simplest mode of *deformation* of a nuclear surface. Within this approximation, the spherical harmonic  $Y_0^0$  is constant, which would imply that any non-vanishing values for  $\alpha_{00}$  will correspond to the change in radius of the nucleus. This kind of excitation is also called *breathing mode* of the nucleus [1, 3]. The energy required for this kind of excitation mode is very large, since it implies a compression of the nuclear matter. As a result, this mode is irrelevant in the low-lying excited spectra of atomic nuclei.

**Dipole mode** Corresponds to  $\lambda = 1$ . In reality, this type of mode does not manifest itself as a deformation of the nucleus, but rather as a shift of the

nuclear center of mass. In the lowest order  $\lambda = 1$ , the shift is in fact a translation of the entire nucleus, and it does not represent an actual nuclear excitation.

**Quadrupole mode** Excited modes that correspond to  $\lambda = 2$ . These are the most important collective excitations that take place inside the nucleus. The loss of axial symmetry, triaxial deformations, and other shape-specific transitions that happen within the nucleus are mostly described (and very accurately) via the quadrupole effects.

**Octupole mode** This corresponds to the next increasing value of  $\lambda = 3$ , representing the main asymmetric excitations of a nucleus with states of negative-parity. The specific shape of a nuclear system governed by octupole deformations is similar to that of a pear.

**Hexadecupole deformations** Excitations which correspond to  $\lambda = 4$ . Within the nuclear theory, this is considered the highest angular momentum which can still provide relevant information for the nuclear phenomena that are studied. Currently, there is no clear evidence for pure excitations with hexadecapole nature, however, these excitations seem to have a major role in the admixture to quadrupole excitations for the ground-state shape of heavy nuclei [3].

The multipole deformations for the cases  $\lambda = 1, 2, 3$  and  $\lambda = 4$  discussed above are pictorially shown in Fig. 2.1. Excitations with higher angular momentum than the mentioned ones have practically no application within the study of atomic nuclei. Moreover, one can also see that there is an intrinsic limitation on the maximal value of  $\lambda$ , which dictates the smallness of the individual bumps of the surface (see Fig. 2.1). These bumps are described by the spherical harmonics  $Y_\lambda^\mu$ , and they decrease in size with increasing values of  $\lambda$ , but with the physical limitation given by the size of the nucleon diameter.

### 2.1.4 Quadrupole Deformation

One of the most important excitation modes (vibrational degrees of freedom) is the quadrupole deformation, corresponding to  $\lambda = 2$ . In the case of pure quadrupole



FIGURE 2.1: Graphical representation of the first few modes of excitations of the nuclear surface. The figure is taken from Ref. [3].

deformation, the nuclear surface will be given by the following expression:

$$R(\theta, \varphi) = R \left( 1 + \sum_{\mu} \alpha_{2\mu} Y_2^{\mu}(\theta, \varphi) \right). \quad (2.8)$$

From this expression, the term  $\alpha_{00}$  is of second order in  $\alpha_{2\mu}$  and it can be neglected further on. This term also reflects the conservation of volume [3, 4]. The real and independent degrees of freedom from the above expression are:  $\alpha_{20}$ , the real and imaginary parts of  $\alpha_{21}$ , and the real and imaginary parts of  $\alpha_{22}$ , respectively.

More insight in regard to the quadrupole shape of the nucleus can be achieved if one expresses  $R$  in terms of Cartesian coordinates. The spherical harmonics will attain a new form, depending on the Cartesian components of the unit vector pointing in a direction defined by  $(\theta, \varphi)$ :

$$\xi = \sin \theta \cos \varphi, \quad \eta = \sin \theta \sin \varphi, \quad \zeta = \cos \theta, \quad (2.9)$$

with the condition  $\xi^2 + \eta^2 + \zeta^2 = 1$ . With the expressions of the spherical harmonics as functions of  $(\xi, \eta, \zeta)$ , the nuclear radius will change accordingly (Cartesian expression  $R = R(\xi, \eta, \zeta)$ ). A relationship between the Cartesian components and the spherical ones for the deformation can be also obtained if one writes all coefficients  $\alpha_{2\mu}$  as functions of  $\alpha_{ij}$  (with  $i, j = \xi, \eta, \zeta$ ). Since the Cartesian deformations can be regarded as closely related to a stretch/contraction of the nucleus in a given direction, a first interpretation of the physical meaning behind the parameters  $\alpha_{2\mu}$  can be established:

- $\alpha_{20}$ : describes the stretching of the  $z$  axis with respect to the  $y$  and  $x$  axes.
- $\alpha_{2-2}$  and  $\alpha_{22}$ : give the relative length of the  $x$  axis compared to the  $y$  axis. Moreover, it also gives the oblique deformation in the  $x - y$  plane.
- $\alpha_{2-1}$  and  $\alpha_{21}$ : describe an oblique deformation, but with respect to the  $z$  axis.

With the set of parameters defined above, the shape and orientation of the nucleus can have arbitrary values (the coefficients  $\alpha_{2\mu}$  are mixing the shape and orientation), thus making the parametrization somewhat problematic. In order to fix that, the geometry can be changed if one considers the *principal axis system* (the PA reference system is a coordinate system in which the moments of inertia associated with the nucleus are diagonal). When using this reference frame, the number of parameters is still unchanged, however their physical significance becomes clearer. By denoting the new coordinate system with primed letters, nuclear radius will be described as a function  $R = R(\xi', \eta', \zeta')$ , with the conditions that  $\alpha'_{ij} = 0$ ,  $i \neq j$ . The condition will further imply that the newly expressed parameters ( $\alpha'_{2\mu}$ ) have the following form:

$$\begin{aligned}\alpha'_{2\pm 1} &= 0 , \\ \alpha'_{2\pm 2} &\equiv a_2 , \\ \alpha'_{20} &\equiv a_0 ,\end{aligned}\tag{2.10}$$

where the conveniently denoted terms  $a_2$  and  $a_0$  are some functions that depend on the Cartesian components  $\alpha_{\xi,\xi}$ ,  $\alpha_{\eta,\eta}$ ,  $\alpha_{\zeta,\zeta}$ . From this set of equations the physical significance of the five real and independent parameters is clearer:

- $a_0$  is indicating the stretch of  $z'$  axis w.r.t. the  $x'$  and  $y'$  axes.
- $a_2$  is indicating the asymmetry between the lengths of  $x'$  and  $y'$  axes, respectively.
- the three *Euler angles*  $\Theta = (\theta_1, \theta_2, \theta_3)$ . These angles will determine the orientation of the PA system  $(x', y', z')$  with respect to the laboratory-fixed frame  $(x, y, z)$ .

One can now clearly see the advantage of working within the PA system: rotation and shape vibration degrees of freedom can be completely separated. A change

in the Euler angles will result in a pure rotation of the nucleus (without changing its shape), while a change in shape will be affected exclusively by the  $a_0$  and  $a_2$  parameters. If  $a_2 = 0$ , then the nucleus has a shape with axial symmetry around the  $z$  axis (equal axis lengths along the  $x$  and  $y$  directions).

Another way of describing the excitations of quadrupole type is to adopt the parameters introduced by A. Bohr [5]. These two parameters can be viewed as a set of polar coordinates in the space generated by  $(a_0, a_2)$  and they are defined as:

$$\begin{aligned} a_0 &= \beta_2 \cos \gamma , \\ a_2 &= \frac{1}{\sqrt{2}} \beta_2 \sin \gamma , \end{aligned} \quad (2.11)$$

where the numeric factor  $\frac{1}{2}$  was added such that the following relation holds true:

$$\sum_{\mu} |\alpha_{2\mu}|^2 = \sum_{\mu} |\alpha'_{2\mu}|^2 = a_0^2 + 2a_2^2 = \beta_2^2 . \quad (2.12)$$

It is worth mentioning that the Eq. 2.12 is rotationally invariant, having the same value in the laboratory and the principal axes systems.

Now that the shape of the nucleus (i.e., the nuclear surface radius  $R$ ) can be described consistently with via the parameters defined in Eq. 2.11, one can calculate the stretching of the nuclear radius along any of the directions is given in terms of  $(\beta, \gamma)$  as follows:

$$\delta R_k = \sqrt{\frac{5}{4\pi}} \beta \cos\left(\gamma - \frac{2\pi k}{3}\right) . \quad (2.13)$$

#### 2.1.4.1 Axial quadrupole deformations

Using this set of new coordinates, the expression of the nuclear radius for axially quadrupole-deformed nuclei is given as:

$$R(\theta, \varphi) = R_0 (1 + \beta_2 Y_2^0(\theta, \varphi)) . \quad (2.14)$$

In Eq. 2.14, the parameter  $\beta_2$  is called the *quadrupole deformation parameter*, and its value dictates whether the nucleus is *oblate* -  $\beta_2 < 0$  (i.e., a flattened sphere), *prolate* -  $\beta_2 > 0$  (i.e., an elongated sphere, like a rugby ball), or *spherical* -  $\beta_2 = 0$ .

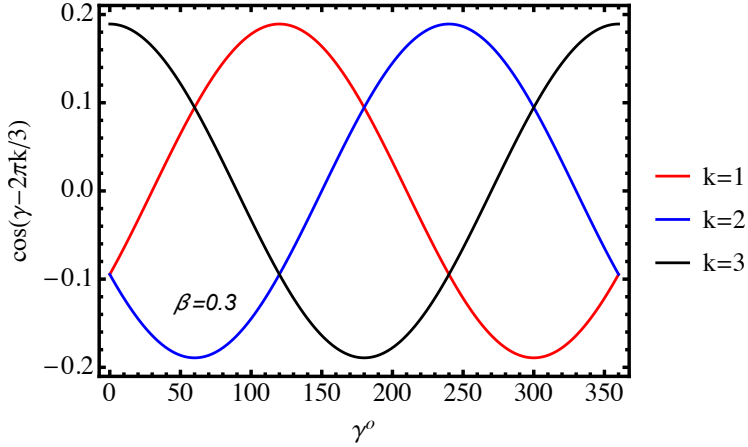


FIGURE 2.2: A graphical representation with the stretching of the nuclear axis  $\delta R_k$  for  $k = 1, 2, 3$ , corresponding to the increase in axis lengths along the  $x$ ,  $y$ , and the  $z$  directions, respectively. The representation used an arbitrary value for the quadrupole deformation  $\beta_2 = 0.3$ . Figure was reproduced according to the calculations done in [3].

The nuclear shapes that are characterized only by  $\beta_2$  (i.e.,  $\gamma = 0$ ) have shapes that correspond to spheroids. These shapes are axially symmetric, meaning that they only have one deformed axis. For the spherical case  $\beta_2 = 0$ , all three axes have the same lengths, meaning that the shape of the nucleus is in fact a sphere.

For the axially-symmetric quadrupole deformations, the parameter  $\beta_2$  can be related to the axes of the spheroid via the formula [3]:

$$\delta R_k = \sqrt{\frac{5}{4\pi}} \beta_2 \cos\left(\gamma - \frac{2\pi k}{3}\right) , \quad (2.15)$$

with  $k = 1, 2, 3$  indices that correspond to each of the three principal axes  $x'$ ,  $y'$ , and  $z'$ , respectively. The stretching of the nuclear axis in a particular direction (denoted by  $k$  in the above formula) varies according to the change in  $\gamma$ , for a fixed value of  $\beta_2$ .

Taking a look at Fig. 2.2, one can see the variations of the three axes with  $\gamma$ . When  $\gamma = 0^\circ$  the nucleus is elongated along the  $z'$  axis, but the  $x'$  and  $y'$  axes are identical (the prolate case) - axial shape. As  $\gamma$  increases, the  $x'$  axis grows, while the other two axes decrease in size, making a region with *triaxial shapes* - all three axes are unequal in magnitude. Symmetry is reached again at  $\gamma = 60^\circ$ , however the  $x'$  and  $z'$  axes are equal this time but longer than  $y'$  axis, making the nucleus look like a flattened shape (the oblate case) - axial shape. This pattern is repeated every  $\gamma = 60^\circ$ , where axial shapes emerge, with alternating prolate/oblate shapes.



FIGURE 2.3: Beta-gamma plane divided into six regions. The first part, delimited from  $\gamma = 0^\circ$  to  $\gamma = 60^\circ$  can be considered as the representative one, while the others can be reproduced from this interval.

It is possible to summarize the various nuclear shapes that can occur with the help of a diagram within in the  $(\beta, \gamma)$  plane. The repeating pattern of the nuclear shapes is graphically represented in Fig. 2.3. One can see that the oblate axially symmetric shapes that occur at  $\gamma = 60^\circ, 180^\circ$  and  $300^\circ$  are identical, and only the axes naming scheme differs. The triaxial shapes are also repeated each  $60^\circ$ .

Regarding the characteristics of Fig. 2.3, the triaxial regions have basically identical shapes, only the axes orientations are different. Moreover, the associated Euler angles are also different, leading to the conclusion that identical physical shapes - including the space orientation - can be represented by different sets of deformation parameters  $(\beta, \gamma)$  and Euler angles.

#### 2.1.4.2 Non-Axial quadrupole deformations

Besides the nuclei characterized by a *spheroidal* shape, where two of the three principal axes have the same length and the quadrupole deformation parameter

$\beta_2$  is the key parameter that describes this kind of shapes, there are also *triaxial* nuclei (or non-axial deformed nuclei).

The triaxial shapes are defined by the  $\gamma$  degree of freedom: the parameter which describes the asymmetry between the length of the three axis of the nucleus (e.g., it describes a stretching along an axis that is perpendicular to the symmetry axis). The nuclear radius for the axially-asymmetric quadrupole deformations is given by:

$$R(\theta, \varphi) = R_0 \left( 1 + \beta_2 \cos \gamma Y_2^0(\theta, \varphi) + \frac{1}{\sqrt{2}} \sin \gamma (Y_2^2(\theta, \varphi) + Y_2^{-2}(\theta, \varphi)) \right), \quad (2.16)$$

which is different from Eq. 2.14. As it was already mentioned, the values  $\gamma = 0^\circ$  and  $\gamma = 60^\circ$  correspond to symmetric prolate and oblate shapes, respectively. Between these values, the triaxial region exist, with *maximal triaxiality* reached at  $\gamma = 30^\circ$ . The deformation parameters  $(\beta, \gamma)$  are also called the Hill-Wheeler set [6].

In Eq. 2.16, the spherical harmonics are expressed as follows:

$$\begin{aligned} Y_2^0(\theta, \varphi) &= \frac{1}{4} \sqrt{\frac{5}{\pi}} (3 \cos(\theta)^2 - 1) , \\ Y_2^2(\theta, \varphi) &= \frac{1}{4} e^{2i\varphi} \sqrt{\frac{15}{2\pi}} \sin(\theta)^2 , \\ Y_2^{-2}(\theta, \varphi) &= \frac{1}{4} e^{-2i\varphi} \sqrt{\frac{15}{2\pi}} \sin(\theta)^2 , \end{aligned} \quad (2.17)$$

and substituting these terms in  $R(\theta, \varphi)$ , Eq. 2.16 will become [1, 7]:

$$R(\theta, \varphi) = R_0 \left[ 1 + \sqrt{\frac{5}{16\pi}} \beta \left( \cos \gamma (3 \cos \theta^2 - 1) + \sqrt{3} \sin \gamma \sin \theta^2 \cos 2\varphi \right) \right]. \quad (2.18)$$

Regarding the nuclear shapes that were described in Fig. 2.3, the redundancies of the  $(\beta, \gamma)$  variables are:

- for  $\beta_2 > 0$  the nucleus is *prolate* for  $\gamma = 0^\circ, 120^\circ, 240^\circ$ .
- for  $\beta_2 > 0$  the nucleus is *oblate* for  $\gamma = 60^\circ, 180^\circ, 300^\circ$ .

- for  $\gamma = 0^\circ, 180^\circ$ , the symmetry axis is the  $z$ -axis of the intrinsic frame
- for  $\gamma = 120^\circ, 300^\circ$ , the symmetry axis is the  $x$ -axis of the intrinsic frame
- for  $\gamma = 60^\circ, 240^\circ$ , the symmetry axis is the  $y$ -axis of the intrinsic frame

#### 2.1.4.3 Lund Convention

The so-called Lund convention [7] somewhat solves this repetitiveness, by selecting a rotational axis according to the set of rules described below:

- The quadrupole deformation parameter  $\beta_2$  is always positive:  $\beta_2 \geq 0$
- The rotation around the smallest axis ( $s$ -axis) implies the constraint on the triaxiality parameter  $0^\circ \leq \gamma \leq 60^\circ$ .
- The rotation around the longest axis ( $l$ -axis) implies the constraint on the triaxiality parameter  $-120^\circ \leq \gamma \leq -60^\circ$ .
- The rotation around the medium/intermediate axis ( $i$ -axis) implies the constraint on the triaxiality parameter  $-60^\circ \leq \gamma \leq 0^\circ$ .

Fig. 2.4 aims at depicting the mechanism behind the Lund convention. The graphical representations organized in Table 2.1 show the possible nuclear shapes, depending on the number of deformation axes; namely, if there is only one deformation axis, then the nuclear shape is *axial-symmetric* (oblate or prolate) and if there are two deformation axes, then the nucleus is *triaxial* (axially-asymmetric).

#### 2.1.4.4 Alternative description of the quadrupole deformation

Considering the Lund convention and the Eq. 2.15, one can re-write the set of stretching values as follows:

$$\frac{R_x - R_0}{R_0} = \sqrt{\frac{5}{4\pi}} \beta_2 \cos \left( \gamma - \frac{2}{3}\pi \right), \quad (2.19)$$

$$\frac{R_y - R_0}{R_0} = \sqrt{\frac{5}{4\pi}} \beta_2 \cos \left( \gamma - \frac{4}{3}\pi \right), \quad (2.20)$$

$$\frac{R_z - R_0}{R_0} = \sqrt{\frac{5}{4\pi}} \beta_2 \cos \gamma. \quad (2.21)$$

$$(2.22)$$

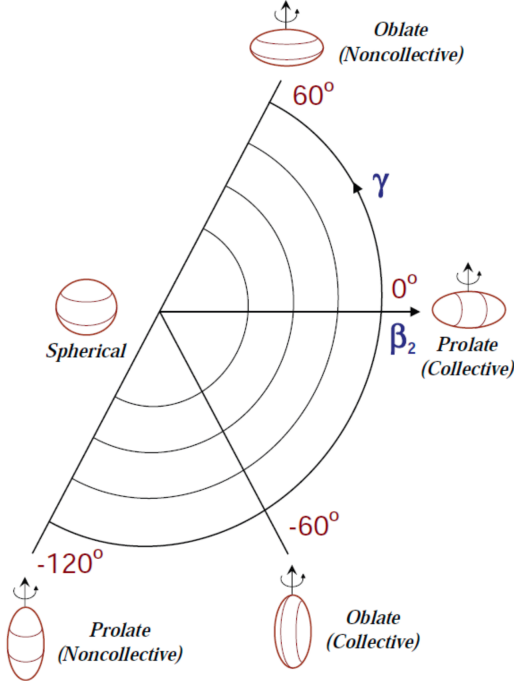


FIGURE 2.4: Representation of the nuclear shapes in the  $(\beta, \gamma)$  plane, using the Lund convention [7] previously discussed. The figure was taken from the work of Matta [8].

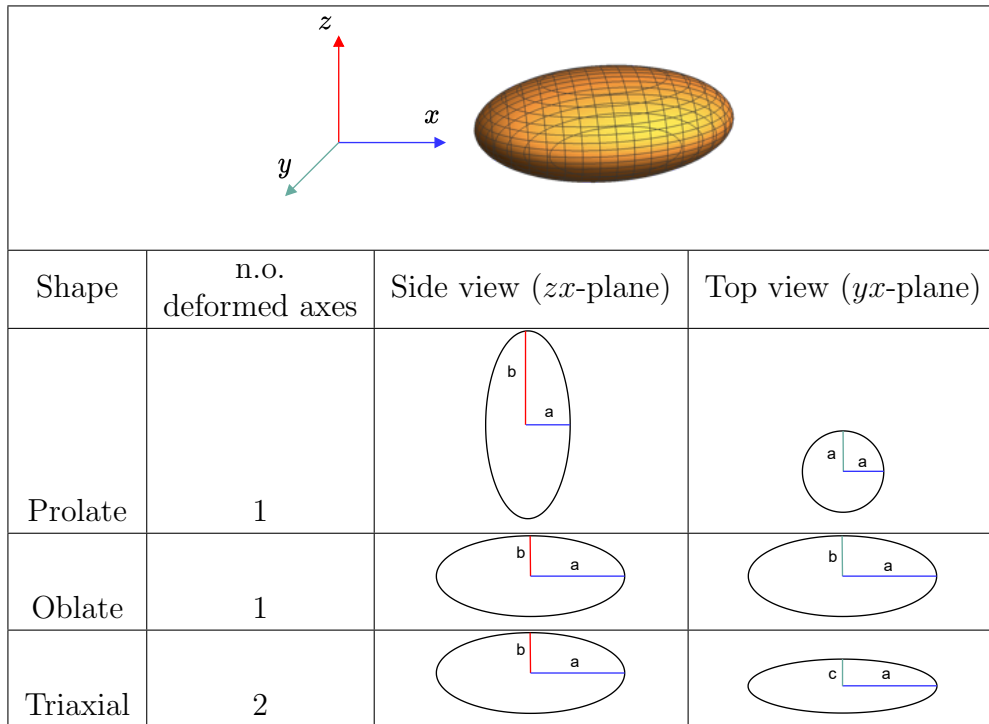
For the axially symmetric deformation (i.e.,  $\gamma = 0$ ), the quadrupole parameter  $\beta_2$  can be derived as follows:

$$\beta_2 = \frac{4}{3} \sqrt{\frac{\pi}{5}} \frac{\tilde{R}}{R_0} , \quad (2.23)$$

where  $\tilde{R} = (R_z - R_x)$  is the difference between the major ( $R_z$ ) and minor ( $R_x$ ) axes of the ellipsoid. This equation for  $\beta_2$  shows how for oblate deformations,  $\beta_2 < 0$  (implying that  $R_z < R_x$ ), while for prolate deformations  $\beta_2 > 0$  (implying that  $R_z > R_x$ ). Within literature, usual values for  $\beta_2$  range from 0.2 - 0.3 (known as *normal deformations*) to 0.4 - 0.6 (known as *superdeformations*).

Another possible description of the nuclear deformation that is specific to small deformations, is given in terms of the parameter  $\epsilon_2$ , with the connection to  $\beta_2$  via the formula [9]:

$$\epsilon_2 \approx \frac{\tilde{R}}{R_0} = \frac{3}{4} \sqrt{\frac{5}{\pi}} \beta_2 = 0.946 \beta_2 . \quad (2.24)$$



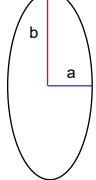
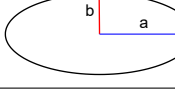
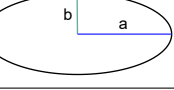
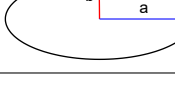
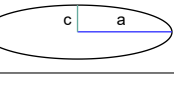
Shape	n.o. deformed axes	Side view ( $zx$ -plane)	Top view ( $yx$ -plane)
Prolate	1		
Oblate	1		
Triaxial	2		

TABLE 2.1: Deformed ellipsoidal shapes of the nuclei. A generic ellipsoid is shown at the top of the table. The parameters  $a$ ,  $b$ , and  $c$  represent lengths of differing magnitude of the nuclear ellipsoid.

### 2.1.5 Nuclear Shapes and Softness

Regarding Table 2.1, a discussion about the implications of the nuclear shapes in terms of some specific phenomena is necessary. Indeed, the shell-model (which will be briefly discussed in the next chapter) considers the motion of the individual nucleons, that are *confined* in nucleonic orbitals, where each nucleon will occupy an orbit with a quantized value of angular momentum. The interpretation of the gamma-ray spectra of different nuclei can be properly described through the excitations if individual nucleons between different orbits, but only for nuclei that are near closed shells. Unfortunately, the same cannot be said about nuclei that lie far from a shell closure, where tools like *Collective Model - C.M.* [1] help understand the properties of these nuclei. One can see that any additional nucleon to the closed shells will imply a departure from the spherical view of a nucleus, with deformations along one of the axes of that nucleus. With the help of C.M., the energy spectrum of many nuclei can be understood and described in terms of 1) a rotation around an axis that is perpendicular to the deformation axis, but also in terms of a 2) motion of the nucleus as a whole (i.e., collective behavior) in tandem

with one coming from a single nucleon (i.e., single-particle behavior). As an example, nuclei in the region  $N = 82$  were extensively studied, and the properties of a given nuclide are not only determined by the specific orbital occupied by valence nucleons (e.g., proton orbitals such as  $s_{1/2}$ ,  $h_{11/2}$  or neutron orbitals such as  $f_{7/2}$ ,  $h_{9/2}$ ), but also the proportion of each shell that is filled with protons and neutrons, respectively. The nuclei in this closed shell  $N = 82$  region are considered as perfect examples of evolutions from the single-particle motion, and the evolution to a collective behavior can be emphasized around the *midshell* at  $N = 104$ . These misspell nuclei have a deformation that is present along only one axis: *axially symmetric*. Every orbital will cause the nucleus to change its shape towards either a prolate or an oblate one. The change in prolate/oblate type of deformation will depend on the value of the quadrupole moment [10], quantity used to evaluate the so-called Nilsson levels [11] (a detailed discussion about the Nilsson orbitals will be made in the following chapter), or Nilsson diagrams: single-particle energies as a function of nuclear deformation. The slope of a Nilsson level is related to the expectation value of the quadrupole moment, via the expression [7]:

$$\frac{de_k}{d\beta} = - \langle j | q | j \rangle \quad (2.25)$$

with  $e_k$  representing the energy of the single-particle state  $|j\rangle$ ,  $\beta$  is the deformation, and  $q$  is the quadrupole operator. Each nucleon that occupies an orbit with a given slope will contribute to an overall deformation: one nucleon that occupies a downward sloping orbital which for positive  $\beta$  will drive the nucleus to a prolate shape, while the other type of nucleon that occupies an upward sloping orbital will drive the nucleus to an oblate shape. The competition between these two polarizing effects will result in the axial asymmetry.

In triaxial nuclei (*axially-asymmetric*), a number of low-lying nuclear configurations can exist, leading to different shapes. When the nucleus has a dynamic degree of triaxiality (via the  $\gamma$  deformation parameter), it is said to be a  *$\gamma$ -soft nucleus*.

$\gamma$ -soft nuclei tend to exist when both the protons and neutrons occupy the top and bottom of their shells, respectively. The opposite also holds [12] true. The conditions for  $\gamma$ -soft nuclear deformations are realized, for example, in  $N \approx 90$  nuclei, where the Fermi surfaces are located near the top of the proton shell ( $h_{11/2}$ ) and bottom of the neutron shell ( $i_{13/2}$ ).

It is interesting that a single nucleus does not necessarily holds a single fixed shape. If the potential energy surface (PES) is relatively flat with respect to the triaxiality parameter  $\gamma$  (meaning that there is no constrain with regards to the minimum value of  $\gamma$ ), the shape can oscillate within an interval of deformation. Such a feature characterizes the  $\gamma$ -softness of the nucleus itself.

# Chapter 3

## Nuclear Models

### 3.1 Introduction

In the following, it is worth to make a discussion about the nuclear models that are used by theoreticians in order to describe phenomena that are specific to rotating nuclei and high-spin regime. Since the focus of this work emerges from a *class* of properties that usually apply to the high-spin region (but this does not necessarily also imply a high-energy region), it makes sense to give an insight in the tools that fit the best the underlying effects.

#### 3.1.1 Shell model

The fact that an atomic nucleus can have a structure that behaves rather similarly as its *parent* (i.e., the atom) in terms of changing the number of constituents, has been enforced by the experimental observations that were done across time. The sharp and discrete discontinuities of nuclear properties, such as the nucleon separation energy, point to the fact that nucleus can be explained through the existence of *shells*. Some examples of observations which indicate this are:

- When adding a nucleon to a nucleus, there are certain places where the *binding energy* of the next nucleon becomes considerably smaller than the previous one.

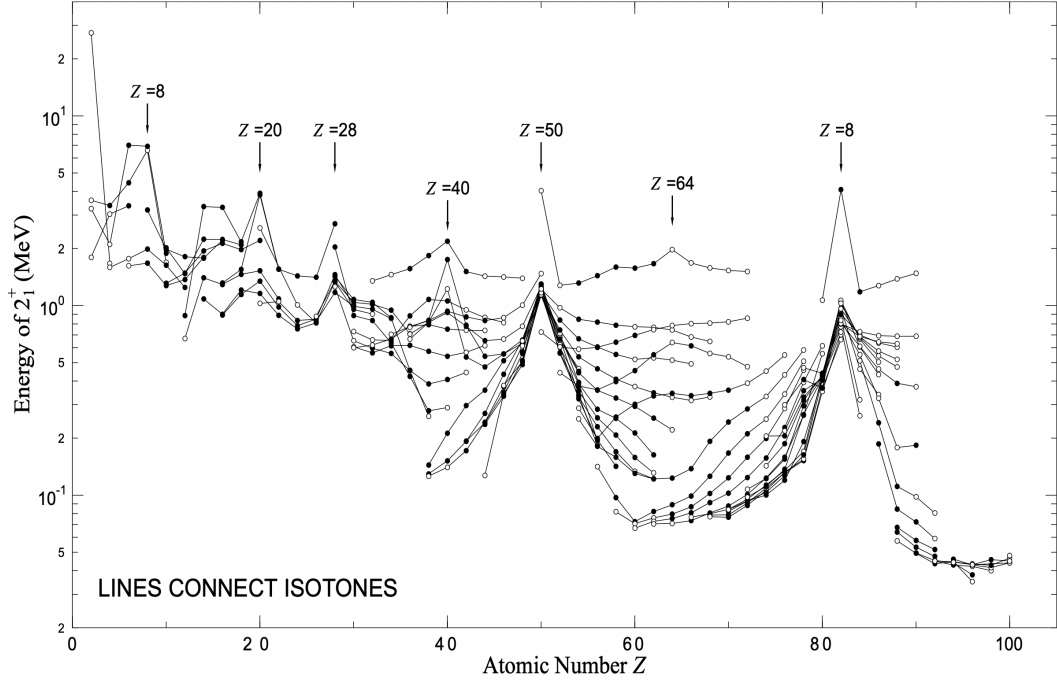


FIGURE 3.1: The first excited energy states  $2^+$  of nuclei with even  $Z$  and  $N$  graphically represented with respect to the proton number. Each line represents a set of isotopes. Figure taken from Ref. [8].

- Separation energies for both the protons and neutrons suffer drastic changes, having strong deviations from the predictions of the semi-empirical mass formula [13], the discontinuities being represented by major shell closures (complete filling) [14].
- The neutron absorption cross-section has a substantial decrease in value at the neutron magic numbers
- Great abundance of nuclides where  $Z$  and  $N$  are magic numbers.

The sudden discontinuities occur at specific values of the proton  $Z$  and neutron  $N$  numbers: these are called *magic numbers*. Currently, these magic numbers correspond to  $Z$  or  $N = 2, 8, 20, 28, 50, 82, 126$ , and they represent the so-called major shells. There are also two *weakly magic numbers*: 40 and 64.

One can examine the values for the first excited states  $2^+$  that are shown in Figs. 3.1, 3.2. Indeed, these values show some peaks, each peak corresponding to a particular magic number.

The shell model starts from the basic assumption that the nucleus is a *mean-field potential*, that is a potential for which the motion of a single nucleon is caused by

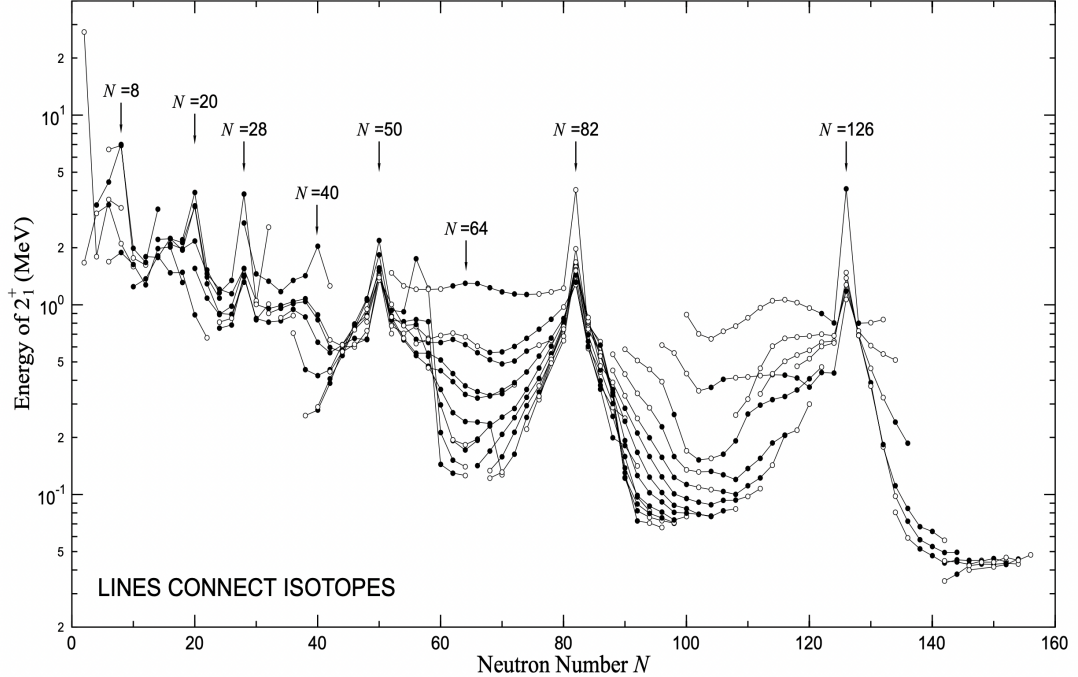


FIGURE 3.2: The first excited energy states  $2^+$  of nuclei with even  $Z$  and  $N$  graphically represented with respect to the neutron number. Each line represents a set of isotopes. Figure taken from Ref. [8].

all the other nucleons (the nucleon is moving inside an average potential generated by all the other constituents of the nucleus). Of course, all the nucleons that are under the influence of such a mean field potential occupy the energy levels which correspond to a series of (sub)shells that agree with the Pauli exclusion principle. Having a general expression for the potential that properly reproduces all the magic numbers (and the observed nuclear properties) is the main goal.

Since the model starts from the concept of independent (non-interacting) particle motion within an average potential, finding each energy will be equivalent of solving the Schrödinger equation:

$$-\frac{\hbar^2}{2m} \nabla^2 \psi_i(r) + V(r) \psi_i(r) = e_i \psi_i(r) \quad (3.1)$$

where  $e_i$  represents the energy (eigenvalue) and  $\psi_i$  represents the wave-function (eigenstates), while  $V(r)$  is the nuclear potential whose expression must be evaluated.

The choice of  $V(r)$  will be dictated by the reproduction of various experimental data (such as nuclear saturation, scattering, nuclear reactions, and so on). For the motion of an independent particle, an obvious first attempt would be the *simple*

*harmonic oscillator* (SHO), which has the known expression:

$$V(r) = \frac{1}{2}m(\omega_i r)^2 , \quad (3.2)$$

with  $\omega_i$  as the frequency of the basic harmonic-like motion of the particle in the nucleus. With Eq. 3.2, the motion of the nucleon has a straightforward expression:

$$\frac{\hbar^2}{2m}\nabla^2\psi_i(r) + \frac{1}{2}m(\omega r)^2\psi_i(r) = e_i\psi_i(r) . \quad (3.3)$$

This Schrödinger equation has its energy eigenvalues under to form:

$$e_N = \left(N + \frac{3}{2}\right)\hbar\omega , \quad (3.4)$$

where  $N$  is the number of oscillator quanta which describes each major shell (also called the *principal quantum number*). One should keep in mind that such an expression is typical for a three-dimensional and isotropic harmonic oscillator. The principal quantum number  $N$  is furthermore defined as:

$$N = 2(n - 1) + l , \quad (3.5)$$

with  $n$  and  $l$  being the *radial* quantum number and *orbital angular momentum* quantum number, respectively, taking values  $n = 1, 2, 3, \dots$  and  $l = 0, 1, 2, \dots, n - 1$ . In this first approximation, all the levels with the same principal quantum number  $N$  are *degenerate*, with a maximal degeneracy given by  $2(2l+1)$ . However, by using only the SHO term as the expression of  $V(r)$ , only the first three magic numbers are reproduced, meaning that some additional term(s) might be needed in order to consistently obtain the series of magic numbers.

A next step is to use the fact that the experimentally observed short range of the strong nuclear force: the steepness of the SHO can be corrected with an *attractive* term proportional to  $l$ -squared. This acts as a centrifugal term which provides an angular momentum barrier, lifting the degeneracy between the levels with the same principal quantum number  $N$  and different values for the orbital angular momentum  $l$ . This SHO+ $l^2$  step is still not enough though. The last step is to add a so-called *spin-orbit* coupling term of the form  $\vec{l} \cdot \vec{s}$ . This term comes from the consideration that the nucleon-nucleon interaction has a spin dependence, and the potential depends on the intrinsic spin  $s$  ( $\vec{s}$ ) and the orbital angular momentum  $l$

( $\vec{l}$ ) of a nucleon. Since  $\vec{j} = \vec{l} + \vec{s}$ , two possible states emerge from a single value of  $l$  (depending on whether  $\vec{s}$  is parallel or anti-parallel to  $\vec{l}$ ). The final expression of the terms SHO+ $\vec{l}^2$ + $\vec{l} \cdot \vec{s}$  will consist in the *Modified Harmonic Oscillator* (MHO).

$$V(r) = \frac{1}{2}(\omega r)^2 + B \vec{l}^2 + A \vec{l} \cdot \vec{s}. \quad (3.6)$$

For the sake of simplicity, the centrifugal term will be denoted within formulas without the vector symbol. Since the intrinsic spin of a nucleon is  $s = 1/2$ , for a given value of  $l$ , there can be two values for the *total angular momentum* (a.m.)  $j = l \pm 1/2$ : one for each spin orientation with respect to the direction of the orbital a.m. Moreover, for each value of  $l = 0, 1, 2, 3, 4, \dots$ , there is a similar notation  $l = s, p, d, f, g, \dots$ , respectively. Regarding the spectroscopic notation, usually, the value of  $j$  is considered as a subscript;  $nl_j$  (for example  $1p_{1/2}$  and  $1p_{3/2}$ ). What it is worth mentioning is that for high enough shells, there can be splittings between  $j + 1/2$  and  $j - 1/2$  that are large enough to lower the  $j + 1/2$  state from one oscillator shell  $n$  to one located below  $n - 1$ . These types of levels are called *intruder states* and they have opposite parity  $\pi = (-1)^l$  with respect to the shell that these levels will occupy.

Going back to the expression of the  $\vec{l} \cdot \vec{s}$  term from Eq. 3.6 and denoting it with  $V_{ls}(r)$ , it is shown by Casten [9] that its contribution to the total potential can be regarded as a surface effect. Due to this, its form can be expressed as a function that depends on the radial coordinate as such [9]:

$$V_{ls}(r) = -a_{ls} \frac{\partial V(r)}{\partial r} \vec{l} \cdot \vec{s}, \quad (3.7)$$

where  $V(r)$  is the expression for a central potential and  $a_{ls}$  is a strength constant.

Now that an expression for the nuclear potential that is able to reproduce all the magic numbers has been formulated, it is also possible to formulate the total energy of a single-particle within the average potential that is generated by all the other nucleons within the nucleus. Thus, the Hamiltonian of this simple system (the modified oscillator) can be formulated as such:

$$\begin{aligned} H &= -\frac{\hbar^2}{2m} \nabla^2 + V_{\text{SHO}} + (l^2)_{\text{term}} + (\vec{l} \cdot \vec{s})_{\text{term}} = -\frac{\hbar^2}{2m} \nabla^2 + V_{\text{MHO}}, \\ H &= -\frac{\hbar^2}{2m} \nabla^2 + \frac{1}{2}m(\omega r)^2 + Bl^2 + A\vec{l} \cdot \vec{s}. \end{aligned} \quad (3.8)$$

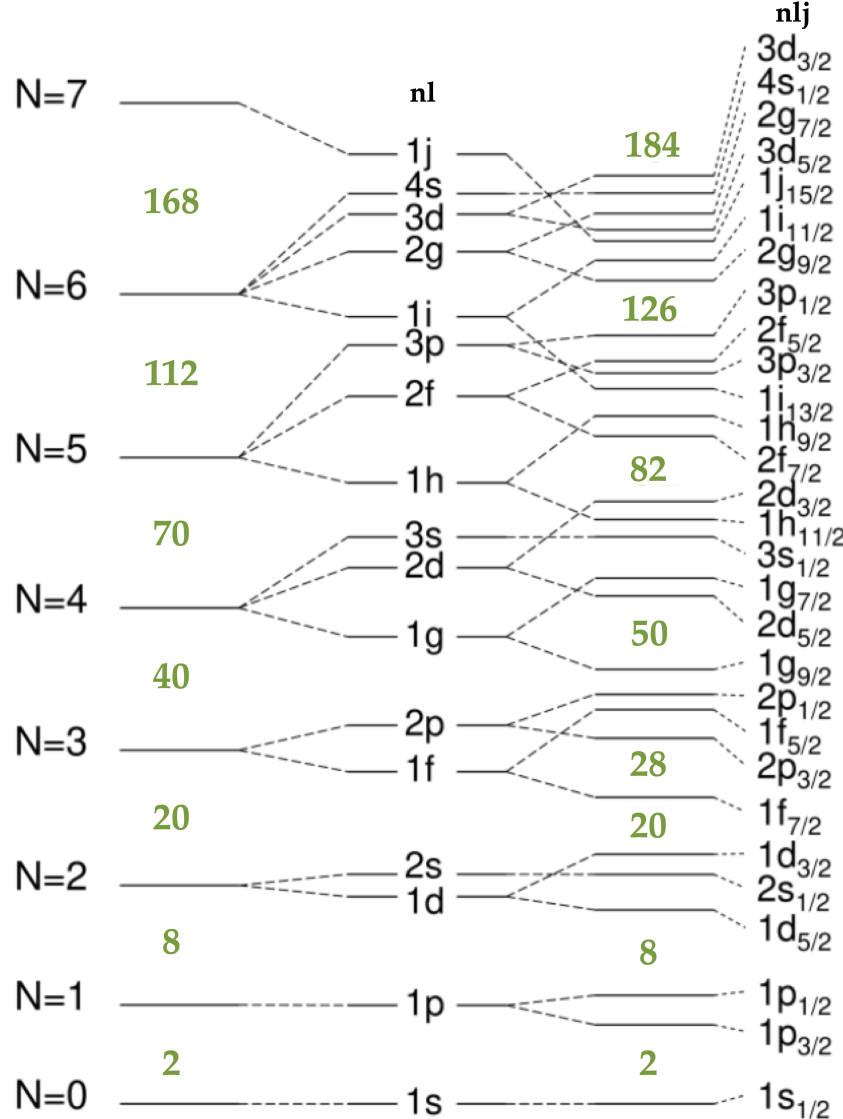


FIGURE 3.3: The energy levels obtained via calculation of the shell model potential using the simple oscillator (SHO), the SHO amended with a centrifugal term  $l^2$ , and finally the modified oscillator (MHO) that contains a spin-orbit term. The ‘correct’ magic numbers are the ones in the right-most column.

Figure is adapted from Refs. [8],[14].

The evolution from each term in the shell-model potential (that is the first approximation as a SHO, then SHO+ $l^2$ , and finally SHO+ $l^2 + \vec{l} \cdot \vec{s}$  or modified oscillator potential) is illustrated in Fig. 3.3, where it can be seen how each extra term introduces a new degeneracy within the energy states, with the complete reproduction of the magic numbers in the third column. Moreover, the *intruder* levels can be observed, where levels with  $j = l + 1/2$  from a particular  $n$  are so low, that they lie below an  $n - 1$  adjacent level.

Another, more realistic potential that can be used in order to reproduce the specific shell model calculation is the so-called Woods-Saxon potential. Because of the short-range character of the strong nuclear force, it is safe to assume that this potential should behave in the same manner as the density distribution of the nucleons. Since for medium and heavy nuclei, the Fermi-like functions (distributions) are the ones that best fit the experimentally measured data, this potential should have the following form [15]:

$$V_{\text{ws}}(r) = -\frac{V_0}{1 + e^{\frac{r-R_0}{a}}} . \quad (3.9)$$

This mean-field potential contains the terms  $V_0$  that represents the depth of the potential ( $\approx 50$  MeV, in order to reproduce the experimental separation energies for the nucleons), the surface thickness  $a$  (also called the diffuseness parameter, giving information about how fast the potential drops to zero) with a value of approximately 0.5 fm, while  $R_0$  is the nuclear radius with  $R_0 = r_0 A^{1/3}$  and  $r_0 = 1.2$  fm. The nature of this potential is of *central type* and, unfortunately, Eq. 3.9 in its pure form is not enough to reproduce the higher magic numbers. As such, the addition of a spin-orbit term, similarly as in the case of MHO potential, is required [16]:

$$V_{\text{total}} = V_{\text{ws}}^{\text{central}} + V_{ls}(r) \vec{l} \cdot \vec{s} . \quad (3.10)$$

The only good quantum numbers in the case of the WS potential are the total a.m.  $j$  and the parity  $\pi = (-1)^l$ . The expectation value of the spin-orbit term  $\vec{l} \cdot \vec{s}$  can be given as:

$$\langle ls \rangle = \hbar^2 \begin{cases} \frac{l}{2} & \text{for } j = l + \frac{1}{2} \\ -\frac{l+1}{2} & \text{for } j = l - \frac{1}{2} \end{cases} . \quad (3.11)$$

and the spacing between two levels can be furthermore expressed as [16]:

$$\Delta E_{ls} = \frac{2l+1}{2} \hbar^2 \langle V_{ls} \rangle . \quad (3.12)$$

The experimental evidence points to the fact that  $V_{ls}(r)$  is negative, meaning that states with  $j = l - 1/2$  are shifted higher than  $j = l + 1/2$ . Some characteristics of the WS potential are the following:

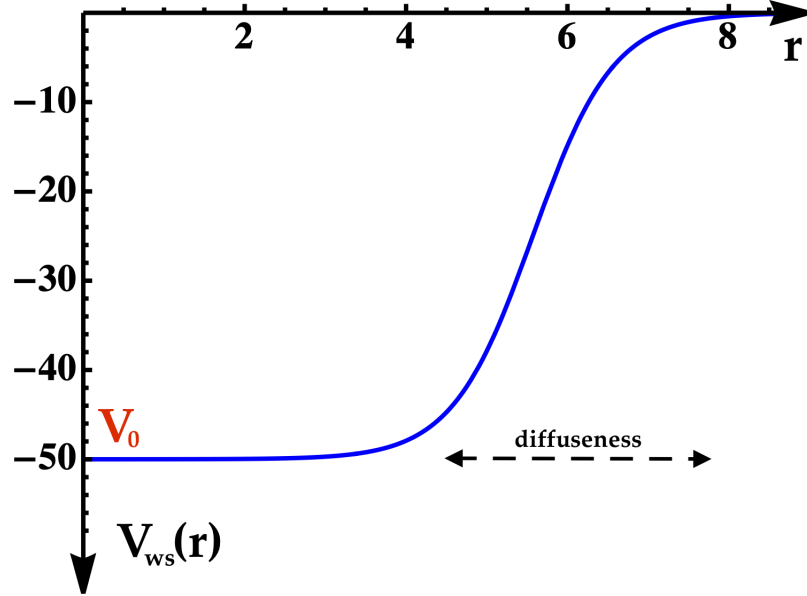


FIGURE 3.4: The shape of the Woods-Saxon potential, defined by Eq. 3.9. The parameters are arbitrarily chosen as:  $V_0 = 50$  MeV,  $R = 5.57$  fm, and  $a = 0.5$  fm.

1. It increases with the increase of  $R$ , meaning that it has an *attractive nature*
2. It flattens out for large enough  $A$  in the center of the nucleus
3. It rapidly goes to zero as  $R$  increases (given by the diffuseness parameter), indicating its short-range nature
4. When  $R = R_0$  (that is for the nucleons near the surface), a large force towards the center of the nucleus is experienced by the these nucleons.

Fig. 3.4 shows the shape of a typical Woods-Saxon potential. Aiming at a final Hamiltonian which describes the motion of the nucleon within the mean-field potential, the formula can be readily obtained:

$$H = -\frac{\hbar^2}{2m} \nabla^2 + V_{ws}^{\text{central}} + (\vec{l} \cdot \vec{s})_{\text{term}}, \quad (3.13)$$

$$H = -\frac{\hbar^2}{2m} \nabla^2 - \frac{V_0}{1 + e^{\frac{r-R_0}{a}}} + A \vec{l} \cdot \vec{s}. \quad (3.14)$$

In addition to the shape of the Woods-Saxon potential, a comparison between it, a SHO, and the square-well-like potential is made in Fig 3.5.

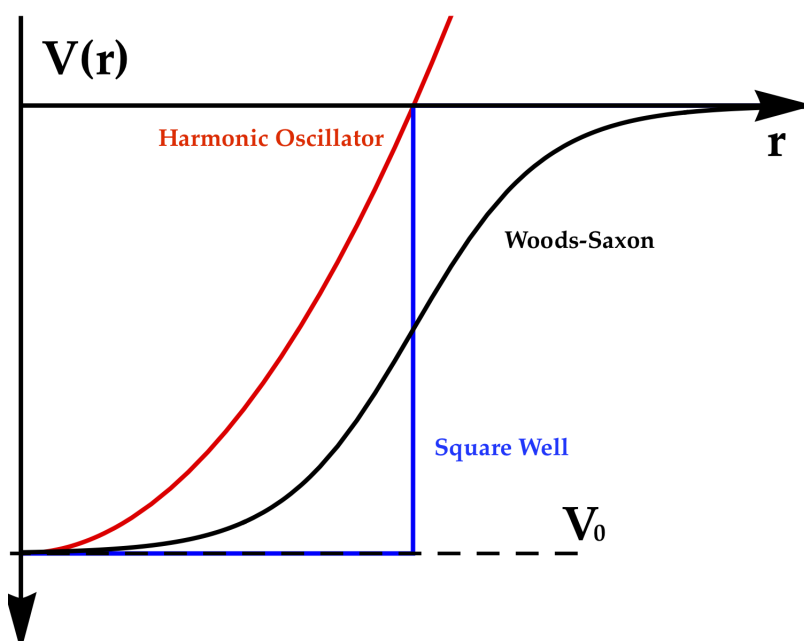


FIGURE 3.5: A schematic representation with the three kind of potentials used to describe the shell model: harmonic oscillator, Woods-Saxon, and for completeness, the square-well.

# Bibliography

- [1] Aage Niels Bohr and Ben R Mottelson. *Nuclear Structure (In 2 Volumes)*. World Scientific Publishing Company, 1998.
- [2] H Morinaga and PC Gugelot. Gamma rays following ( $\alpha$ , xn) reactions. *Nuclear Physics*, 46:210–224, 1963.
- [3] Walter Greiner and Joachim A Maruhn. *Nuclear models*. Springer, 1996.
- [4] Peter Ring and Peter Schuck. *The nuclear many-body problem*. Springer Science & Business Media, 2004.
- [5] Aage Bohr. *Rotational states of atomic nuclei*. Munksgaard, 1954.
- [6] Samuel SM Wong. *Introductory nuclear physics*. John Wiley & Sons, 2008.
- [7] G Andersson, SE Larsson, G Leander, P Möller, Sven Gösta Nilsson, Ingemar Ragnarsson, Sven Åberg, R Bengtsson, J Dudek, B Nerlo-Pomorska, et al. Nuclear shell structure at very high angular momentum. *Nuclear Physics A*, 268(2):205–256, 1976.
- [8] James Till Matta. *Exotic Nuclear Excitations: The Transverse Wobbling Mode in  $^{135}\text{Pr}$* . Springer, 2017.
- [9] R Casten and Richard F Casten. *Nuclear structure from a simple perspective*, volume 23. Oxford University Press on Demand, 2000.
- [10] Michael Christopher Lewis. *Lifetime Measurements of Excited States in  $^{163}\text{W}$  and the Properties of Multiparticle Configurations in  $^{156}\text{Lu}$* . The University of Liverpool (United Kingdom), 2019.
- [11] Ingemar Ragnarsson and Sven Gvsta Nilsson. Shapes and shells in nuclear structure. *Shapes and Shells in Nuclear Structure*, 2005.

- [12] QB Chen, SQ Zhang, PW Zhao, and J Meng. Collective hamiltonian for wobbling modes. *Physical Review C*, 90(4):044306, 2014.
- [13] CF von Weizsäcker. Zur theorie der kernmassen. *Zeitschrift für Physik*, 96(7):431–458, 1935.
- [14] Kenneth S Krane. *Introductory nuclear physics*. John Wiley & Sons, 1991.
- [15] Roger D Woods and David S Saxon. Diffuse surface optical model for nucleon-nuclei scattering. *Physical Review*, 95(2):577, 1954.
- [16] Brian R Martin and Graham Shaw. *Particle physics*. John Wiley & Sons, 2017.